Optics of multiple quantum wells uniaxially stressed along the growth axis

P. Etchegoin
Max-Planck-Institut für Festkörperforschung, Heisenbergstrasse 1, 70569 Stuttgart, Germany
and Cavendish Laboratory, University of Cambridge, Madingley Road, CB3 0HE, Cambridge, United Kingdom

A. Fainstein
Max-Planck-Institut für Festkörperforschung, Heisenbergstrasse 1, 70569 Stuttgart, Germany
and France Telecom, CNET/PAB Laboratorie de Bagneux, B. P. 107, 92225 Bagneux Cedex, France

A. A. Sirenko
Max-Planck-Institut für Festkörperforschung, Heisenbergstrasse 1, 70569 Stuttgart, Germany
and Ioffe Physicotechnical Institute Politekhnicheskaya 26, 194021 Saint Petersburg, Russia

B. Koopmans, B. Richards, P. V. Santos, M. Cardona, K. Totenmeyer, and K. Eberl
Max-Planck-Institut für Festkörperforschung, Heisenbergstrasse 1, 70569 Stuttgart, Germany
(Received 14 August 1995; revised manuscript received 8 February 1996)

Data are presented on in-plane transmission of light and photoluminescence for GaAs/AlAs multiple quantum wells (MQW's) uniaxially stressed along the $\hat{z}=[001]$ growth axis. This stress leads to the simplest possible form of competition between confinement and stress in these microstructures. We show that by measuring the frequency-dependent birefringence in the energy window between the absorption edge of the MQW's and that of the substrate (GaAs), direct information about the competition between uniaxial stress and confinement can be obtained. We find that the inclusion of finite **k** mixing between heavy- and light-hole bands is necessary in order to account for the otherwise very puzzling polarization rules of the luminescence. The piezobirefringence in the transparency region is found to be of the same order of magnitude than that of bulk GaAs.

I. INTRODUCTION

Application of external stresses (hydrostatic,[1] uni- and biaxial) to solids is a well established technique for investigating the physical properties of crystals.[2] The field of semiconductor microstructures has also profited from this technique: several experiments on the optical properties of single and multiple quantum wells (MQW's) under stress have already been reported in the literature.[3–8] Optical experiments in MQW's under uniaxial stress made use of techniques such as photoluminescence (PL), electro- or photoreflectance (PR), photoluminescence excitation spectroscopy (PLE), or, simply, polarized normal reflectance[3–8] to determine the simultaneous effect of confinement and stress (either built in due to lattice mismatch or externally applied) on the hole and electron subbands of the wells. So far, optical experiments have emphasized the case where the uniaxial stress is applied along one of the directions perpendicular to the growth axis (i.e., in the planes of the wells), because of the ease of optical excitation and/or collection from the face perpendicular to that axis. Uniaxial stress in those experiments is thus not collinear with the quantization axis $\hat{z}=[001]$ and, in addition, for some type of samples a built-in biaxial stress component is also present due to lattice mismatch of the structure and the substrate [this is the case of single quantum wells of GaAs grown on Si(001)].[3] If the molecular-beam-epitaxy- (MBE-) terminated face of a microstructure (perpendicular to the growth axis) and the substrate underneath are used to apply an external uniaxial stress, little optical access is left for observing the electronic states in the wells, except from the side of the structure (typically $\ll 1\,\mu$m). There are at least two optical experiments that still function and provide information on the heavy- (hh) and light-hole (lh) splitting in this configuration: (i) transmission of light along the planes (which only works here if the sample is clad and provides a direct measument of the birefringence below the gap[9]), and (ii) photoluminescence; the sample can still be excited from the side and, due to the very high efficiency of the luminescence process, it is actually possible to observe the heavy- and light-hole reemission from the side. In addition, inelastic light scattering experiments for light propagating along the planes of the structure are possible.[10,11]

There are several reasons why this configuration with an external stress along the growth axis is attractive. First of all, from a fundamental point of view the case in which the uniaxial stress is parallel to the growth axis provides the simplest example of competition between confinement and stress. Both effects act along the same axis and produce the same type of symmetry reduction, with respect to bulk GaAs. Both confinement and uniaxial stress along $\hat{z}$ reduce the point group of bulk GaAs from T_d to D_{2d} (ignoring the inequivalence of consecutive interfaces) and an anisotropy between the optical constants of the well for light polarized parallel and perpendicular to $\hat{z}$ (birefringence) is correspondingly introduced. When the two effects operate together, the final result depends on their relative sign. Actually, the confinement energy tends to push the (lh) band to lower energies leaving the (hh) above it, while a uniaxial stress along $\hat{z}$

tends to push the (hh) and (lh) bands in the opposite direction (due to the particular sign of the deformation potentials), giving rise to an effective competition between the two mechanisms [at $\mathbf{k}\neq\mathbf{0}$ the (hh) and (lh) are mixed in a QW, but at $\mathbf{k}=\mathbf{0}$ the identification in terms of the wave functions of the bulk is still exact].

We recently have performed experiments[9] in unstressed samples in which the birefringence of MQW's was directly measured by observing the transmission of light along the planes of the wells through crossed polarizers. The observed dispersion of the birefringence presented a puzzling behavior,[9] with a fairly large background birefringence (birefringence far from the gap). We know now that this was caused by an artifact in the way the data have been analyzed and that an additional experiment is needed to determine this value. This is done here in the manner explained in Sec. II. We found, in addition, further interesting questions which are raised by the piezo-optical response of the MQW's.

The paper is organized as follows. Section II gives the introduction needed for analyzing the data and the experimental setup, the sample preparation, and the experimental results. Section III contains a discussion of the results based on different approaches. Section IV presents the conclusions.

II. EXPERIMENT AND DATA EVALUATION

A. Theoretical overview

The frequency-dependent optical constants below the gap can be understood as arising from two contributions:[12] (i) a dispersionless term (related to virtual direct transitions involving high energy gaps) and (ii) a resonant term which represents the isolated effect of the virtual transitions associated with the first gaps (the lowest one and its spin-orbit partner are normally considered to contribute to the dispersion). Both contributions have actually the same origin (i.e., they can be calculated using the Fermi golden rule and the electric-dipole approximation), but the contributions of the first gaps are isolated from the rest because they are *more resonant* than the others by having the smallest energy denominators in the real part of the dielectric tensor components. They are, therefore, the only ones which are normally treated explicitly in analytic models, leaving the transitions to higher gaps as a dispersionless constant. This approach, using parabolic bands, involves diagonalizing matrices not larger than 4×4 and thus leads to analytic expressions. In bulk GaAs, the lowest absorption edge is defined by a single direct gap at Γ between the degenerate (hh) and (lh) bands and the first Γ_1 conduction band. When measured by light absorption or transmission, for example, the gap is independent of polarization, as expected by symmetry. When a compressive uniaxial stress along [001] is applied, or a well is formed so that confinement takes place along the [001] growth axis, two main effects determine a change in the optical constants below the gap: (i) (hh) and (lh) split at $\Gamma=0$ and (ii) the average gap [from the *center of gravity* of the (hh) and (lh) to the first conduction band] increases. In the case of a uniaxial stress along [001], and due to the sign of the deformation potentials, the (lh) band at Γ is pushed to higher energies than the (hh), while in the case of confinement, and due to the fact that the (lh) is *lighter* in the confinement direction, the (lh) is pushed below the (hh). The mixing of the bands at $\mathbf{k}\neq\mathbf{0}$ and the effects over other bands are of course completely different for the two effects, but, with regard to the (hh)-(lh) splitting at Γ, one may say that confiment has a *similar* effect as a tensile stress. The rest of the band structure is formally very different for the two perturbations and, in particular, band folding produced by confinement is by no means equivalent and cannot be produced by a uniaxial stress. In practice, however, the *new* solids, GaAs under uniaxial stress *or* confined along [001], have dielectric properties which, for optical gaps above the fundamental, can be described as small (but measurable and distinguishable) perturbations of the dielectric function of bulk GaAs.

We now present what is actually expected from the one-electron approximation for the below-gap dispersion of samples under stress and confinement.

The (hh) and (lh) bands come from atomic p-states and can be written as a linear combination of atomic $|X\rangle$, $|Y\rangle$, and $|Z\rangle$ wave functions and hole spinors α, and β as[13]

$$|3/2,+3/2\rangle=\frac{-1}{\sqrt{2}}(|X\rangle+i|Y\rangle)\alpha,$$

$$|3/2,+1/2\rangle=\frac{-1}{\sqrt{6}}(|X\rangle+i|Y\rangle)\beta+\sqrt{\tfrac{2}{3}}|Z\rangle\alpha,$$

$$|3/2,-1/2\rangle=\frac{1}{\sqrt{6}}(|X\rangle-i|Y\rangle)\alpha+\sqrt{\tfrac{2}{3}}|Z\rangle\beta,$$

$$|3/2,-3/2\rangle=\frac{1}{\sqrt{2}}(|X\rangle-i|Y\rangle)\beta, \tag{1}$$

where the functions with $\mathbf{J}=3/2$, $J_z=\pm3/2$ $(\pm1/2)$ represent the heavy (light) hole bands which are doubly degenerate due to time reversal. The (hh) band has no $\hat{z}$ component while the (lh) is more isotropic and has components along all axes. When the two states are split, we are left with a crystal that actually has two gaps depending on polarization. If light polarized along $\hat{z}$ impinges on the crystal, it can only couple to the (lh), while if the light beam is polarized, perpendicular to $\hat{z}$ (i.e. perpendicular to the quantization axis or uniaxial stress) it can couple to both (hh) and (lh) states, and the absorption edge will be defined for this polarization by the lower of the two.[14]

The Hamiltonian of a single well of a MQW in which electrons and holes may be present (eventually in the form of excitons) and on which an external stress may be applied can be written in general as[4,15,16]

$$\hat{H}=\hat{H}_{\rm elec}+\hat{H}_{\rm hole}+\hat{H}_{\rm ex}+\hat{H}_{\varepsilon}, \tag{2}$$

where $\hat{H}_{\rm elec}$ is the electron Hamiltonian taken here in the effective mass approximation,

$$\hat{H}_{\rm elec}=-\frac{\hbar}{2m_e}\nabla^2+V_e(z)+\Delta, \tag{3}$$

$\hat{H}_{\rm hole}$ is the Luttinger-Kohn Hamiltonian[17] for the holes, which describes the appropriate mixing of heavy and light holes according to the three phenomenological Luttinger parameters γ_1, γ_2, and γ_3,

$$\hat{H}_{\rm hole}=-\frac{\hbar}{2m_0}\left(\frac{\gamma_1}{2}k^2-\gamma_2\left[J_x^2-\frac{1}{3}J^2\right]k_x^2+\text{c.p.}\right)$$
$$-2\gamma_3(\{J_x,J_y\}k_xk_y+\text{c.p.})+V_h(z), \tag{4}$$

$\hat{H}_{\rm ex}=-e^2/\epsilon r$ is the Coulomb interaction between electrons and holes, screened through the mean dielectric constant $\epsilon=(1/3)\ \mathrm{Tr}[\epsilon_{ij}]$, and

$$\hat{H}_{\varepsilon}=D_d(\varepsilon_{xx}+\varepsilon_{yy}+\varepsilon_{zz})+\tfrac{2}{3}D_u[(J_x^2-\tfrac{1}{3}J^2)\varepsilon_{xx}+\text{c.p.}]$$
$$+\tfrac{4}{3}D_u'(\{J_x,J_y\}\varepsilon_{xy}+\text{c.p.}), \tag{5}$$

the effective stress Hamiltonian. In Eqs. (3)–(5) the symbols are as follows. m_e is the effective mass of the electrons in the Γ_1 conduction band; $V_e(z)$ is the electron well barrier; Δ is the constant hydrostatic shift of the gap (this shift fixes the energy of the average gap and, indirectly, the effective masses involved in the transitions); m_0 is the bare electron mass; $\mathbf{J}=[J_x,J_y,J_z]$ is the angular momentum operator acting on the wave functions (1); $V_h(z)$ is the hole well barrier; D_d, D_u, and D_u' are the hydrostatic and shear deformation potentials for the valence band; and ε_{ij} is the strain tensor. In (4) and (5), c.p. refers to cyclic permutations of indices. Here we are mainly interested in the simultaneous diagonalization of (4) and (5). We neglect, for the time being, the exchange interaction in (2) to make clear the predictions of the one-electron picture. If the externally applied uniaxial stress X is along the same $\hat{z}$ quantization axis as (4), then (4) and (5) have only diagonal elements in the basis of wave functions (1), implying, automatically, that the stress dependence of the (hh) and (lh) should be linear in X. Writing ε_{ij} in terms of the elastic compliance constants s_{ij} and the stress tensor components $X_{ij}=X\delta_{zz}$ ($\Gamma_1+\Gamma_3$ representations of T_d) and after calculating the diagonal matrix elements for the (hh) and (lh), we obtain

$$\Delta E_{\rm lh}^{\rm hh}=a(s_{11}+2s_{12})X\pm b(s_{11}-s_{12})X \tag{6}$$

for the shifts of the (hh) (+) and (lh) (−) energy levels. In (6) we have $b=(2/3)D_u$ and $a=(D_d+C')$ where C' is the hydrostatic deformation potential that shifts the conduction band in (3) [$\Delta=C'(\varepsilon_{xx}+\varepsilon_{yy}+\varepsilon_{zz})$]. Therefore the (hh) and (lh) *do not mix at* $\mathbf{k}=\mathbf{0}$ and preserve their character for all stresses, having a stress dependence parametrized by two constants a, and b. Equation (6) is the basis for understanding the predictions of the one-electron approximation.

The contributions of higher bands to the optical constants below the gap (the dispersionless term of the birefringence), which strongly affect the optical characteristics of the system, are completely beyond the scope of this model and, in fact, of any analytic calculation. Normally, one must rely on a complete band structure calculation of the optical constants to obtain this term. We shall come back to this problem later. With the linear shifts of the (hh) and (lh) bands as a function of X_{ij} in mind, we turn back to the problem of the birefringence below the gap under stress. For a given applied stress X_{ij}, the real part of the dielectric tensor component for light polarized parallel to the growth axis ($\hat{z}$) of the MQW's, $\epsilon_{\parallel}(\omega)$, below the gap, is given by[12] (in atomic units; $m=\hbar=e=1$)

$$\epsilon_{\parallel}(\omega)=C_{\parallel}-\frac{4\mu_{\rm lh}P_{\rm lh,\parallel}^2}{\omega^2 d}\ln\left[1-\left(\frac{\omega}{\omega_{\rm lh}^g}\right)^2\right], \tag{7}$$

where $\omega_{\rm lh}^g$ is the (lh)-to-Γ_1-electron band energy gap, $P_{\rm lh,\parallel}^2$ the corresponding optical matrix element (squared), $1/\mu_{\rm lh}$ the (optical) effective mass for this transition, d the thickness of the well, and $C_{\parallel}$ a constant representing the background. The second term represents the contribution of the smallest gap to which one can couple [the (lh) in this polarization].[12]

For the other polarization, parallel to the planes of the MQW's, one can couple the electric field of the light beam to both the (hh) and (lh) since, according to (1), both have $|X\rangle$ and $|Y\rangle$ components. Therefore two frequency-dependent logarithmic singularities arise in this polarization and $\epsilon_{\perp}(\omega)$ is given by

$$\epsilon_{\perp}(\omega)=C_{\perp}-\frac{4\mu_{\rm hh}P_{\rm hh,\perp}^2}{\omega^2 d}\ln\left[1-\left(\frac{\omega}{\omega_{\rm hh}^g}\right)^2\right]$$
$$-\frac{4\mu_{\rm lh}P_{\rm lh,\perp}^2}{\omega^2 d}\ln\left[1-\left(\frac{\omega}{\omega_{\rm lh}^g}\right)^2\right], \tag{8}$$

where $\omega_{\rm hh}^g$, $P_{\rm hh,\perp}^2$, and $\mu_{\rm hh}$ are the corresponding [as in (7)] parameters of the (hh)-to-Γ_1-electron band gap. Note that the matrix element to the (lh) gap, in this case $P_{\rm lh,\perp}^2$, is different from the one used in (7), since we are now coupling to the in-plane component of the (lh) wave function (1). The matrix elements, the gaps, and the effective masses are actually not completely independent but related through the $\mathbf{k}\cdot\mathbf{p}$ relation $1/\mu\sim 2P^2/E_{\rm gap}$. The difference between the indices of refraction for the two polarizations (the birefringence) is then obtained from (7)–(8) by means of the expression $(n_{\perp}-n_{\parallel})=(\epsilon_{\perp}-\epsilon_{\parallel})/(\sqrt{\epsilon_{\perp}}+\sqrt{\epsilon_{\parallel}})\sim(\epsilon_{\perp}-\epsilon_{\parallel})/2\overline{n}$ ($\overline{n}=$ mean index of refraction).

B. Data analysis

If the incident light field $\mathbf{E}_{\rm incident}$ is polarized at 45° with respect to the growth axis $\hat{z}$ (in the [$\hat{x}$-$\hat{z}$] plane with $\mathbf{k}\|\hat{y}$) then $\mathbf{E}_{\rm incident}=|E|/\sqrt{2}(\hat{x}+\hat{z})$ and, after traveling a distance l along the planes, is transformed in $\mathbf{E}_{\rm out}=|E|/\sqrt{2}(e^{2\pi n_{\perp}l/\lambda}\hat{x}+e^{2\pi n_{\parallel}l/\lambda}\hat{z})$ due to the birefringence. By analyzing the output light with a polarizer crossed to the original input polarization we get a transmitted intensity proportional to

$$I_{\rm out}\sim I_0\left[1-\cos\left(\frac{2\pi[n_{\parallel}(\omega)-n_{\perp}(\omega)]l}{\lambda}\right)\right]$$
$$=I_0\sin^2\left(\frac{\pi\Delta n(\omega)l}{\lambda}\right), \tag{9}$$

where $\lambda=2\pi c/\omega$ is the wavelength of the light in vacuum. Accordingly, we get oscillations in the transmitted intensity which contain information on the dispersion of the birefringence $\Delta n(\omega)=[n_{\parallel}(\omega)-n_{\perp}(\omega)]$. If the birefringence is dispersionless, then the maxima and minima in the transmission

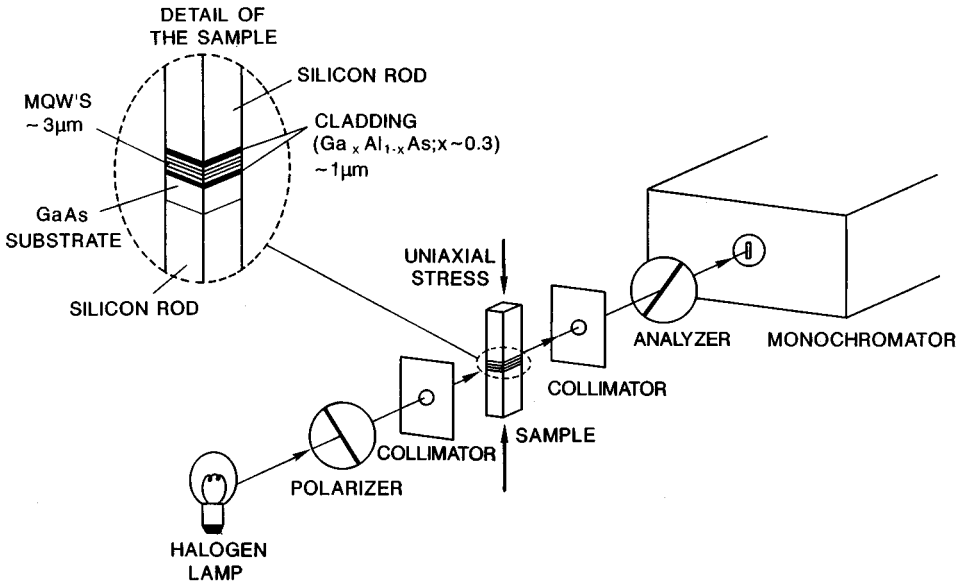

FIG. 1. Schematic view of the experimental setup. The light emited by a halogen lamp is collimated onto the side of the sample by using a pinhole. No lenses are used to avoid multiple angles of incidence due to the convergence of the beam. The sample is glued between two silicon rods and masked on the sides (not shown in the picture) to avoid spurious light going into the monochromator (see text for details and Ref. 18 for a description of the stressing rig). The ''detail of the sample'' shows a MQW with $Al_xGa_{-x}As$ cladding and GaAs substrate, glued in between two [001] silicon rods with a mixture of epoxy and silver powder. The whole arrangement is polished together to obtain smooth surfaces suitable for optics.

are equally spaced in energy ($\propto 1/\lambda$). If not, the maxima and minima shrink or expand depending on whether the birefringence increases or decreases at the resonance, respectively.[9] In analyzing the data with Eq. (9) one is left with N data points (the positions of the peaks) and $N+1$ unknowns [because the ''absolute'' phase of a peak cannot be obtained from (9)]. This can be solved if one assumes that $\Delta n(\omega)$ is dispersionless far from the gap and, therefore, is the same for the first two peaks. A first value for $\Delta n(\omega)$ is extracted from which the rest are then obtained. We found, however, that a small, almost negligible, dispersion can induce large errors in the determination of the first value of $\Delta n(\omega)$ and this turned out to be the cause for the large background birefringence reported in Ref. 9. An additional experiment is needed to obtain an absolute phase for the peaks; we have used for this purpose reflection experiments with a microscope objective and an elasto-optic modulator. We used a combination of measurements with crossed polarizers and the modulator to calibrate the curve for zero stress. Once the first curve is calibrated, the dispersions for all stresses can be obtained.

We have now the basic tools for the discussion of the stress dependence of the birefringence and of the energy position of the (hh) and (lh) as seen in the luminescence.

C. Experimental details and sample preparation

The experiment is based on that reported in Ref. 9 and therefore we keep details to a minimun while emphasizing new features. For the birefringence measurements, transmission of light (parallel to the planes) through crossed polarizers was used. We found it possible to use a halogen lamp as a light source, instead of using a tunable Ti-sapphire laser as in Ref. 9. The lamp housing is placed close to the sample holder of the stressing rig[18] and collimated with a pinhole. A schematic view of the experiment is given in Fig. 1. No lenses are used to focus the light in order to avoid multiple angles of incidence on the first face due to the convergence of the beam (which we found produces an undesirable background in the analyzed transmitted light). The incident beam is polarized at 45° with respect to the growth axis of the sample, along which the uniaxial stress is applied. The output spot is further collimated and analyzed with a crossed polarizer. Finally, the transmitted light is detected by a monochromator with gratings blazed at 1.5 μm and a GaAs photomultiplier. We worked with a resolution of 1.5 cm^{-1}.

We used two samples for our experiments. Sample A is a 300-period GaAs/AlAs (18/16 monolayers) MQW (total thickness $\sim$2.8 μm) clad with two 1.5 μm $Al_{0.7}Ga_{0.3}As$ layers (lower index of refraction in the infrared, below the gap, with respect to that of the MQW) transforming the whole structure into a waveguide for transmission along the planes.[9] This sample has a (hh) gap at room temperature and zero stress of $\sim$1.565 eV and a (hh)-(lh) confinement splitting of $\sim$40 meV. The optical path length of sample A (defined by two cleaved [110] surfaces) was 0.98 mm. Sample B is a 173-period GaAs/AlAs structure (75/85 Å, total thickness $\sim$ 3 μm) with the same type of cladding as sample A. The optical path for the transmission experiments was 1.15 mm, again along [110]. The reasons for using two samples with different confinement energies and therefore different (hh)-(lh) splittings, but similar well/barrier ratio, will become clear soon. For very narrow samples, the approximation of propagation through conventional ray optics breaks down and the transmission has to be analyzed in terms of propagation through electromagnetic modes of the cavity. However, for a sample of our dimensions and with a weak *contrast* of indices of refraction between the cladding and the sample,

we showed in Ref. 9 that ray optics is still valid and only a very small correction ($<0.3\%$) to the optical constants may apply. Further details are given in Ref. 9.

The samples are glued with opaque epoxy to two silicon rods (oriented along [001]) as shown in Fig. 1 (detail of the sample) and the whole arrangement is polished with diamond powder to obtain surfaces suitable for optics. The gap of silicon is well below the region in which we are interested and, therefore, acts naturally as a mask for light not being transmitted through the sample. By measuring in the energy window between the gap of the substrate (GaAs) and the gap of the MQW's ($\sim$1.565 eV for sample *A* and $\sim$ 1.495 eV for sample *B*, at zero stress), the only light that can propagate through the structure comes from the waveguided MQW's. The rest is absorbed either in the substrate or in the silicon rods (consequently there are no strong requirements for the focus on the side of the sample). Additional masking is added to the sides of the samples to avoid spurious reflections getting into the optical path. The whole arrangement is set into the stressing rig[18] and the transmitted light collected into and analyzed by the monochromator.

For the luminescence measurements, we excited the backside of the sample (the one looking towards the monochromator in Fig. 1) with a cw Ti-sapphire laser. The spot has to be adjusted in every measurement to hit the sample, which moves slightly as the uniaxial stress is applied. This prevented a comparison in absolute units for the luminescence taken at two different stresses, since the excitation conditions may slightly vary from one to the other. The excitation energy was set well above the gap of the MQW's (at $\sim$1.75 eV) to avoid resonance effects. No dependence of the measured light on the incident polarization was detected. The signal was collected and detected with the same optical elements as in the transmission experiments, except for a polarization rotator which was set at the entrance of the monochromator to analyze the polarization of the luminescence (parallel and perpendicular to the stress) with the same detectivity and dynamic range as the whole system. All measurements were performed at room temperature.

D. Experimental results

In Fig. 2 we show the in-plane transmission of sample *A* through crossed polarizers, as a function of stress. Several features can be observed. (i) With increasing stress, the point at which the birefringence oscillations [Eq. (9)] vanish moves to higher energies. This reflects the hydrostatic shift of the average gap mentioned in Sec. II A. (ii) The detected intensity of the oscillations becomes weaker in the region, $\sim$1.40 eV and then a small shoulder appears at the lowest photon energies. Note that the spectra have not been corrected for the sensitivity of the spectrometer. The oscillations are weak in this region simply because the photomultiplier attached to our monochromator has a GaAs cathode and has, therefore, low sensitivity near its gap. The small shoulder at even lower photon energies ($\sim$1.385 eV for $X=0$ kbar) corresponds to the situation in which the gap of the substrate (GaAs) has been reached and, accordingly (although the sensitivity of the detector is very weak in this region) there is a sudden increase in the amount of transmitted light through the sample by several orders of magnitude (essentially given by the ratio between the thickness of the whole wafer, sample+substrate, and the thickness of the sample itself, $\sim 10^3$). This shoulder does not contain information on the optical properties of the MQW's but helps in identifying the position of the gap of the GaAs substrate and, consequently, provides an *in situ* probe for the stress. (iii) The number of birefringence oscillations per unit photon energy clearly decreases as the pressure is applied, meaning that the original anisotropy due to confinement is being reduced [see Eq. (9)] by the external uniaxial stress, as expected from the considerations given in Sec. II A.

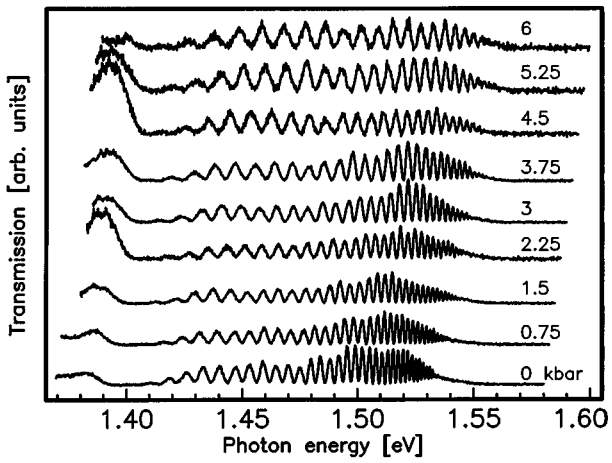

FIG. 2. Transmission of light through crossed polarizers for sample *A* in the experimental configuration shown in Fig. 1. As a function of the externally applied uniaxial stress $X\|[001]$ (labels in kbar) two main effects are observed in the data: (i) the extinction points, i.e., the energies at which the birefringence oscillations [Eq. (9)] vanish, move to higher energies, reflecting the hydrostatic effect of the stress, and (ii) the number of peaks per unit energy is reduced revealing the fact that the birefringence is less under stress than at $X=0$. Note a crossover in the stress dependence of the extinction point around 4.5 kbar. See text for details.

The fact that there are two gaps defined by the (hh) and (lh) transitions and that they couple differently to the incident polarization,[9] while they tend to become closer when the stress is applied, can be proved in the same experiment by simply changing the incident polarization. This is shown explicitly in Fig. 3 for a few stresses: two transmission curves are displayed for each stress $X=0$, 1.5, 3.0, 4.5, and 6.0 kbar. The continuous lines are the same results shown in Fig. 2 but on an expanded scale, close to the extinction point. The incident field, polarized at 45° with respect to $\hat{z}$, can be decomposed into two vectors of the same amplitude, one parallel and one perpendicular to $\hat{z}$. The perpendicular one will couple to the (hh) band, which represents the lowest possible gap it can couple to with that polarization. This component will be absorbed as soon as the first gap is reached. The component of the electric field parallel to $\hat{z}$, however, will only couple to the (lh) which is the first possible gap in this structure that has a wave function with a $|Z\rangle$ component [see (1)]. Hence some light will continue to be transmitted up to the second (lh) gap and above this energy it will be completely absorbed. On the other hand, if the incident polarization is perpendicular to $\hat{z}$ (dotted curves in Fig. 3), two features are expected. (i) there are no birefrin-

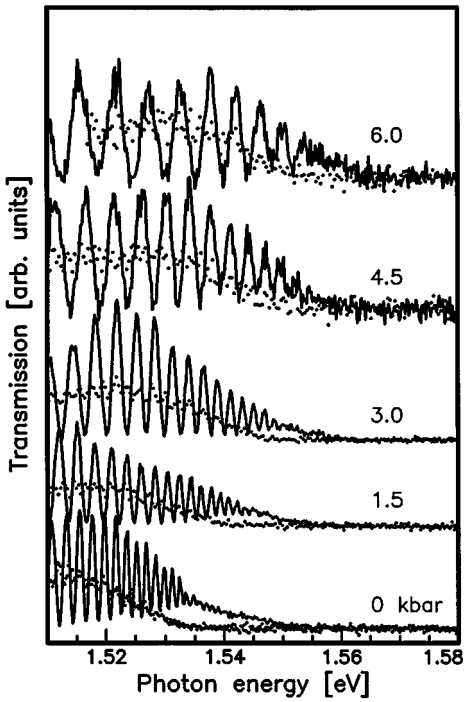

FIG. 3. Transmission of light in sample A for two different incident polarizations, as a function of stress. The solid lines are transmissions for crossed polarizations (as in Fig. 2), while the dotted lines display the transmission for incident polarization perpendicular to [001] (along the MQW planes). In the former, light is transmitted up to the second i.e., e-lh gap, and birefringence oscillations exist, while in the latter light is extinguished at the (hh) gap and no oscillations are observed. Up to 3 kbar, it is clear that two absorption edges exist for the two polarizations and that the two gaps join when the stress is increased. For $X \gg 4.5$ kbar the two extinction points seem to coincide (within the experimental uncertainty), a fact that can be reconciled only if the lowest state is (lh)-like, i.e., if (hh) and (lh) had crossed.

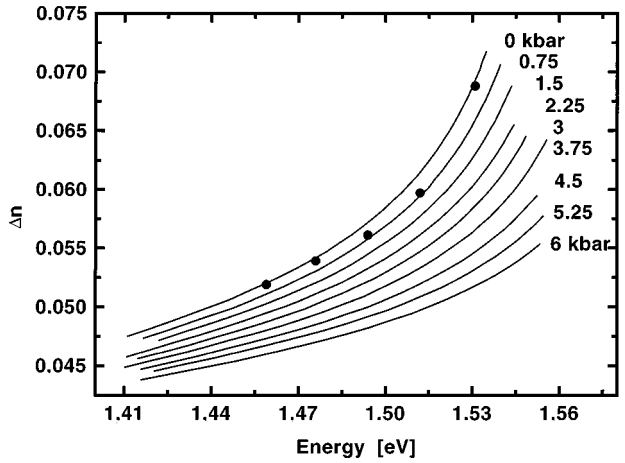

FIG. 4. Analysis of the data in Fig. 2 for sample A. The dots are measurements obtained by microreflectance with an elasto-optic modulator to calibrate the dispersion for $X=0$ kbar. Note that the absolute sign of $\Delta n(\omega)$ cannot be determined from Eq. (9) [$\alpha \cos^2(\Delta n)$], but was measured independently with a compensator. No change in the sign of the dispersion is observed with increasing X.

gence oscillations in this case (the incident polarization is an eigenmode of the propagation of light and the beam leaves the sample without changing polarization), and (ii) light couples only to the (hh) and is wiped out as soon as this energy is reached. There are, therefore, two different absorption edges for the two cases, revealing the presence of the two gaps [(hh)-(lh) splitting]. At $X=0$ kbar, it is clear that the continuous line has non-negligible transmission in the region around ~ 1.535 eV where, at the same time, the other polarization is already extinguished. Note also, as mentioned before, that the extinction point for polarization $\perp \hat{z}$ coincides with the disappearance of the oscillations for 45° polarization. By the same token, it is clearly seen in Fig. 3 (at least for pressures up to ~ 3 kbar) that the two absorption edges approach one another as a function of the applied stress, in addition to the general (hydrostatic) shift of both of them. At 4.5 and 6 kbar the positions of the gaps are less clear and, actually, it looks as if there is a single gap which moves more slowly than the extrapolation of the stress dependence of the extinction point taken from the low stress measurements. This tendency can also be seen with the naked eye in Fig. 2 where there is a crossover in the behavior of the extinction point around 4.5 kbar (it moves approximately linearly up to 4.5 kbar and beyond it shifts very little). This fact, i.e., a change in the shift of the extinction point, together with the data of Fig. 3 which suggest the same gap for both polarizations above $\sim$ 4.5 kbar, can be understood if we assume that the crossing between (hh) and (lh) occurs around this stress [the deformation potential of the (lh) is smaller and this would explain the weaker stress dependence of the extinction point above $\sim$ 4 kbar and, at the same time, since the (lh) has all components $|X\rangle$, $|Y\rangle$, and $|Z\rangle$, a single lowest energy gap exists irrespective of polarization].

From Fig. 2, the dispersion of the birefringence can be obtained. The results of the analysis[19] of the data in Fig. 2 are given in Fig. 4, where $\Delta n(\omega)=[n_{\perp}(\omega)-n_{\parallel}(\omega)]$ is plotted as a function of ω for different uniaxial stresses $X \| [001]$. The calibration points obtained from reflection[19] measurements using an elasto-optic modulator[20] at $X=0$ kbar are also shown in Fig. 4: their scatter around the $X=0$ line enables us to estimate error bars of $\sim 2\%$ for $\Delta n(\omega)$. Figures 5 and 6 complement the analysis for this sample. In Fig. 4, it is clearly seen that the uniaxial stress has two main effects on the birefringence: (i) the low energy side of the curves decreases, and (ii) the curvature close to the absorption edge for each stress (resonant part) becomes weaker as X is increased. The latter is in accordance with what is expected in the one-electron picture, i.e., the stress pushes the (hh) and (lh) bands together (opposing the effect of the confinement at $X=0$) and therefore the MQW's look *more optically isotropic as the stress is applied*. The former effect, however, is harder to understand by simple considerations because it partly involves a change of the background or Penn gap of the MQW's which is only accessible through a numerical calculation based on the band structure, as explained before. It can, however, be compared approximately to the value for bulk GaAs in the transparency region as we shall show later.

In Fig. 5 we show the effect of the stress on the dispersion of Δn, by subtracting the background and, at the same time, normalizing the energy scales to the extinction points (to

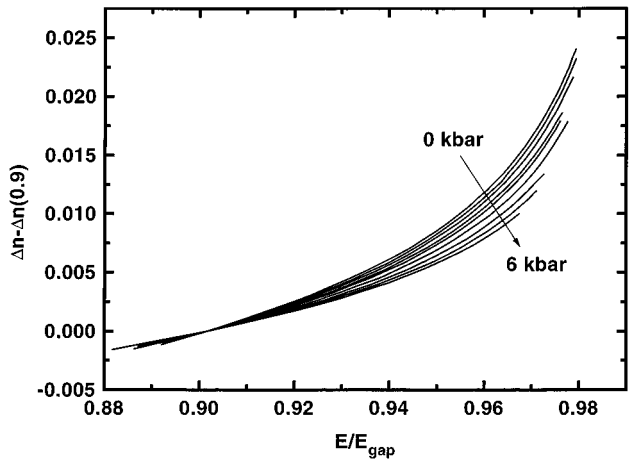

FIG. 5. The data of Fig. 4, but rescaled (in order to compensate for the hydrostatic shift of the gaps) and with the birefringence Δn_0 (0.9) subtracted. The effect of the stress *on the resonant part of the birefringence* is clearly shown here. Note that the dispersion becomes smaller as a function of X (direct competition between confinement and stress), but no inversion in the sign of the dispersion can be seen up to 6 kbar. This is apparently in contradiction with the interpretation of Figs. 2 and 3 in which a change in the deformation potential of the extinction point and a single lowest gap seem to exist above $\sim$4.5 kbar, suggesting that the (hh)-(lh) crossing had occured. See text for further explanations.

correct for the average hydrostatic shift). While the uniaxial stress *reduces* the dispersive part continuously, no change in its *sign* can be observed up to 6 kbar. This can be readily deduced from the raw data (Fig. 2) which show oscillations that become denser *for all stresses* as the gap is approached. Note that this is in contradiction with the expectations of the theory in Sec II A, in view of the apparent crossing between (hh) and (lh) discussed before (Figs. 2 and 3). This point will be discussed further below.

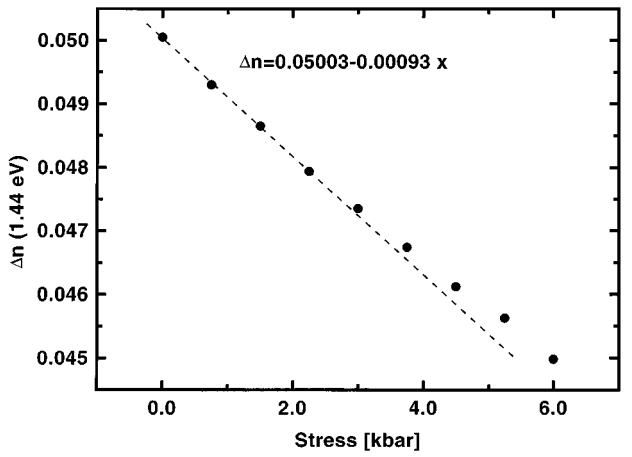

FIG. 6. Stress dependence of the low energy part (background birefringence) taken from Fig. 4. A linear behavior is observed, and the slope of the fit gives a value of $\sim -0.000\ 94\ \text{kbar}^{-1}$; i.e., similar in magnitude to that of bulk GaAs. The effect of the stress on the average gaps of bulk GaAs and GaAs MQW's are roughly the same. A small departure from the linear behavior is observed at large stresses.

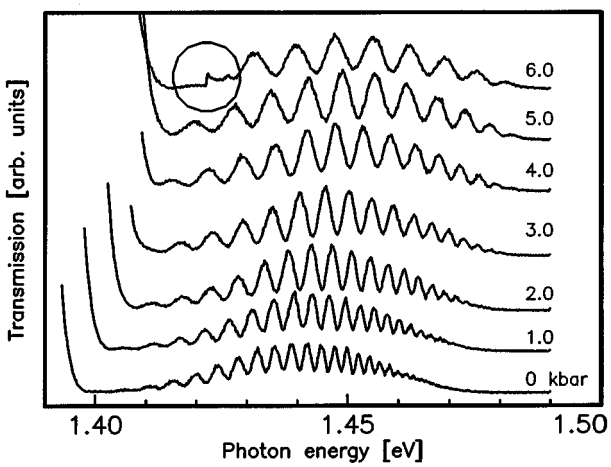

FIG. 7. Transmission for sample B as a function of $X\|[001]$. The birefringence cannot be obtained from here using Eq. (9) because the whole energy window is already in the dispersive part resonant with the gap. The smaller energy window is a direct consequence of the smaller confinement. Two things can be observed: (i) a continuous reduction in the number of peaks per unit energy (perfectly consistent with a birefringence which is less dispersive as a function of X, but does not change sign, as in Figs. 4 and 5 for sample A), and (ii) a crossover in the stress dependence of the extinction point around 2.5–3 kbar. The peak highlighted by the circle represents the moment at which the sample broke because of the stress. See text for details.

In Fig. 6 we plot the stress dependence of the birefringence at fixed photon energy $\sim$1.45 eV to illustrate approximately the effect of the applied stress on the average (Penn) gap. Strictly speaking, the effect on the Penn gap has to be looked at in a region where $\Delta n(\omega)$ is dispersionless, which is not the case at 1.45 eV according to Fig. 2. This is, however, the lowest energy we can measure. Note that the stress dependence is linear, and that the slope of a linear fit ($\sim -0.000\ 94\ \text{kbar}^{-1}$) is roughly the order of magnitude of the piezobirefringence of bulk GaAs in the dispersionless part.[21]

Since an inversion of the birefringence dispersion cannot be obtained in sample A, although the experimental features do suggest that a crossing between (hh) and (lh) occurs, the obvious step is to measure a sample with a smaller confinement and, therefore, to bring the (hh)-(lh) crossing to lower stresses. This is the reason for the measurements on sample B. The transmission of sample B is shown in Fig. 7 for different stresses. Note that the energy window left for this measurement (between the gap of the MQW's and that of the substrate) is much smaller than in Fig. 2, as expected, because of the smaller confinement. The smallest photon energies measured in Fig. 7 lie already where the dispersion of the birefringence is important (no region of constant separation between successive peaks can be identified from the data), and, therefore, it is not possible to extract the birefringence using Eq. (9). Measurements with the modulator have not been performed for this sample. Nevertheless, two important features can be observed in Fig. 7: (i) There is no apparent change of sign in the dispersion of the birefringence (the number of oscillations per unit energy diminishes smoothly up to 6 kbar; a situation similar to that found in

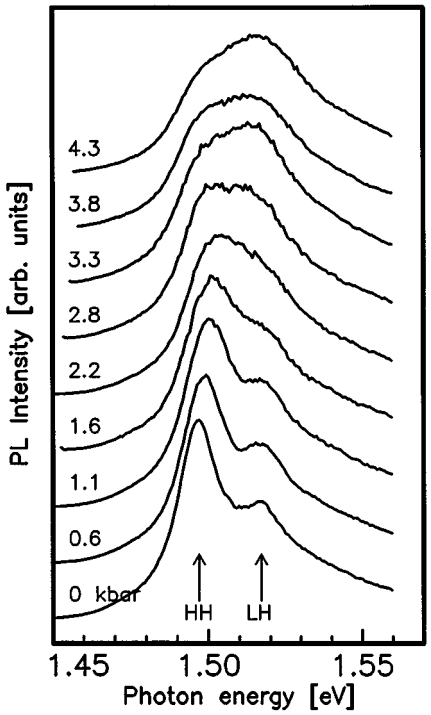

FIG. 8. Luminescence of sample B, detected along $\hat{z}$ under nonresonant excitation. Emission of the (hh) exciton is observed although it should be forbidden at $\mathbf{k}=\mathbf{0}$. The peaks tend to join around 2.5 kbar and the whole picture can be better understood by assuming an anticrossing of the levels instead of the crossing suggested by the one-electron theory. The anticrossing requires an interaction between (lh) and (hh) brought about by the exchange in (2). Similar results hold for sample A.

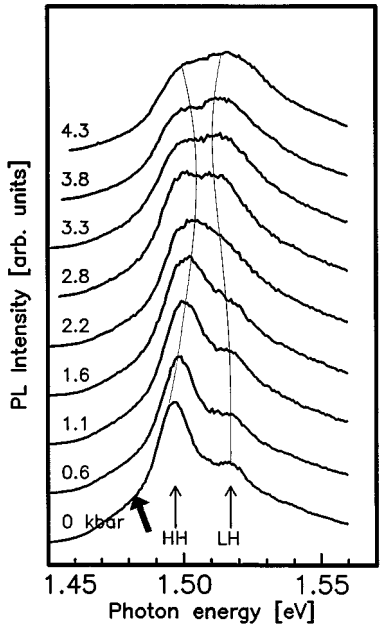

FIG. 9. Same as Fig. 8 but for $(\hat{x},\hat{y})$ polarization. Essentially the same phenomenology is observed as in sample A, except that (hh) and (lh) tend to join at a lower stress (around 2.5 kbar) and the (lh) emission looks more quadratic as a function of X than in sample A. Note the presence of a weak shoulder (thick arrow) on the low energy side of the (hh) peak at $X=0$ when compared with the $\hat{z}$ polarization. The latter is attributed to impurity-mediated recombination. The solid lines give an idea of how the positions of the peaks are fitted with a linear stress dependence for the (hh), a quadratic one for the (lh), and Cho's Hamiltonian (Ref. 13) with an exchange interaction of 5 meV. See text for further details.

sample A and shown in Figs. 4 and 5) and (ii) there is also a crossover in the behavior of the extinction point, which occurs now at lower stresses than for sample A ($\sim$3 kbar). Again, as in sample A, the extinction point rises linearly up to the crossover and then remains almost constant.

The polarized luminescence from the side of sample B is shown in Figs. 8 and 9. We discuss the data for sample B because they are less inhomogeneously broadened than those for sample A. The observed patterns, however, are similar for both samples. The $\hat{z}$ polarized luminescence in Fig. 8 shows emission involving the (hh). In addition, there is a shoulder below the (hh) in the $(\hat{x},\hat{y})$-polarization (thick arrow in Fig. 9) which is only seen through careful comparison of the low energy side of the peak between Figs. 8 and 9. The (hh)-(lh) peaks merge at about $\sim$3 kbar, exactly where the crossover in the stress dependence of the extinction point is observed for sample B (Fig. 7). The main result displayed in Figs. 8 and 9 [besides the apparent anomaly in the $\hat{z}$ emission of the (hh)] is that the (hh) and (lh) seem to *anticross* around 3 kbar. The anticrossing would mean an interaction between the (lh) and (hh) bands. Through this interaction, some of the observed features, including the $\hat{z}$ emission of the (hh) are explained semiquantitatively in a rather natural manner. This is the subject of the next section, where all the results are analyzed in the light of the above mentioned anomalies of the one-electron model. The reason for using two samples with different confinements but the same well-barrier ratio is to avoid in these results any contribution from local fields (as predicted macroscopically by boundary conditions), which was one of the speculations in Ref. 9.

III. DISCUSSION

It is clear from the results presented above that the one-electron approximation and $\mathbf{k}=\mathbf{0}$ optical transitions predict a picture which faces serious difficulties in explaining, even qualitatively, the experimental facts. Here we propose a plausible explanation but make clear that a full band structure calculation of the piezo-optical response, including approximations beyond the one-electron theory, is needed for quantitative confirmation. To this end, we first give a list of facts which can be read from the data and suggest possible explanations.

(i) The $\hat{z}$ emission of the (hh) in Fig. 8 (also observed in sample A although forbidden in the one-electron picture at $\mathbf{k}=\mathbf{0}$) can be explained by considering finite $\mathbf{k}$ exciton recombination. In fact, even without invoking the presence of stress, confinement brings about the proper mechanism for mixing (hh) and (lh) at finite in-plane $\mathbf{k}$. The mixing is small for small $\mathbf{k}$ but the emission of the lowest energy level is always enhanced in luminescence. In other words, if an energy level is the lowest possible, even if it is weakly dipole allowed, it will display a luminescence comparable to other (strongly allowed) levels above it, simply because of the absence of other relaxation channels. Evidence that the exact

selection rules of the bands at Γ are violated has also been found in the in-plane PL emission of doped quantum wells under uniaxial stress.[21]

(ii) The *anticrossing* between (hh) and (lh) in Figs. 8 and 9 is in apparent contradiction with the *crossing* [Eq. (6)] predicted by the one-electron theory. This contradiction can be easily removed by going beyond this approximation and including the exchange Hamiltonian in (2). The most general Hamiltonian including exchange and stress has been given by Cho[13] and predicts not only exchange interaction of (hh) and (lh) even at $\mathbf{k}=\mathbf{0}$ but also the existence of *stress-induced linear-in-***k** *terms*. The latter is of little consequence for our experiments because we always observe the emission along a cleaved [110] surface but it does make a difference for emission along [100] in which the (hh) and (lh) wave functions are further mixed by this term. If the (hh) and (lh) are split by the action of the confinement potential, then the off-diagonal linear-in-**k** interaction induced by the stress[13] produces a mixing of the two bands proportional to k and a splitting proportional to k^2. The latter may become linear in **k** if the confinement splitting is reduced by the stress and the (hh) and (lh) become degenerate. In practice the degeneracy is lifted by the exchange interaction.

(iii) A quantitative fit of the dependence on stress of the peak positions shown in Figs. 8 and 9 with the $\mathbf{J}=1$ states derived from Cho's Hamiltonian (Table VIII in Ref. 13) leads to a reasonable (although somewhat large) exchange interaction (analytic plus dipole-dipole[13]) of ~ 5 meV. This figure, obtained by fitting the experiment, is not very accurate because the peaks are very broad. The large value obtained from the fit can also be explained by a small in-plane built-in stress, which is not included in the model. On the other hand, the shift of the (lh) luminescence of sample B faces difficulties when comparing it with (6). By following with a naked eye the positions of the (hh) and (lh) for different stresses in Fig. 8, for example, one can see that, although the stress dependence of the (hh) is fairly linear (and can be fitted with the deformation potentials $a\sim 8$ eV and $b\sim 1.6$ eV in accordance with calculations[24] and other experiments[7]), the (lh) has a quadratic stress dependence. The (lh) is expected to have a quadratic redshift because of its interaction with the split-off band which also has a $\hat{z}$ component. This also happens for bulk GaAs.[22] Normalizing the (lh)-split-off gap and taking the experimental data from Ref.22 we find a quadratic coefficient of $\sim -0.000\,34$ eV/kbar^2, while that observed in the experiment is three times larger.

(iv) The shoulder in the luminescence of the (hh) at zero stress (thick arrow in Fig. 9) is observed about 20 meV below the (hh) maximum in the in-plane ($\hat{x}$-$\hat{y}$) polarization only. Since our samples are very likely to contain small amounts of shallow impurities (C or/and Si), this shoulder is attributed to the electron-to-(hh)-acceptor luminescence.

(v) The one-electron picture presented in Sec. II A predicts a change in the sign of the dispersion when the (hh) and (lh) are inverted. We clearly see the anticrossing in sample B, less clearly in sample A, but neither the transmission data in Fig. 2 nor the experiments in Fig. 7 seem to indicate that the dispersion of the birefringence actually changes its sign. These facts can still be qualitatively reconciled if we consider the uncompensated effect of the second, third, etc., minibands. In other words, *even if the (hh) and (lh) are degenerate due to the external stress, the solid is still birefringent below the gap because the second, third, etc., minibands are still not degenerate at that stress*. The sign of this birefringence contribution is the same as that expected for the lowest minigap at low stresses. One may argue that by moving closer to the first gap resonance with the (hh) and (lh) should eventually show up and the sign of the birefringence should be inverted even when the second, third, etc., minibands are still not compensated. However, we cannot get sufficiently close to the first gap in transmission because the absorption increases sharply close to the gap. The uppermost photon energy at which we still see oscillations in Figs. 2 and 7 is still rather far from the gap. Therefore it looks as if the *confinement effects* are able to keep the same sign for the dispersion below (and sufficiently far) from the first gap even when the (hh) and (lh) reverse.

Finally, (vi) the birefringence at one of the lowest possible energy we can measure (~ 1.45 eV) is of the same order of magnitude of the one of bulk GaAs in the long wavelength limit far from the gap.[20] Note, however, that according to Fig. 4, the curves are far from being dispersionless at ~ 1.45–1.45 eV and therefore a comparison with the dispersionless piezobirefringence of GaAs bulk is somewhat artificial. In fact, the sign obtained in Fig. 6 is opposite to the long wavelength result of bulk GaAs because we are above the isotropic point[20] of the piezobirefringence. The piezobirefringence of bulk GaAs and confined GaAs forming a well are expected to be similar for energies well below the gap but a direct comparison of the two will require measurements below the gap of the substrate (~ 1.40 eV) which cannot be done by transmission as in Figs. 2 and 7 but may be possible with microreflectance.

IV. CONCLUSIONS

We have investigated the simultaneous effect on the optical properties of MQW's of confinement and stress along the same axis. The gross features of the experimental results can be reasonably well understood by assuming mixing of the (hh) and (lh) excitons and optical emission with finite **k**. We demonstrate the remarkable property of inverting the (hh) and (lh) bands without inverting the sign of the dispersion of the birefringence, a fact probably related to the uncompensated effect of other minibands, above the fundamental gap. We obtained the same order of magnitude in the piezobirefringence below the gap at ~ 1.45 eV in *confined* GaAs when compared with the bulk. The puzzling behavior of the background birefringence reported in Ref. 9 was solved here by an independent determination of the absolute phase in the transmission spectra. Calculations of the dispersion of the birefringence and the piezo-optical response of MQW's going beyond the one-electron approximation are not available; they may be needed for a quantitative explanation of these phenomena.

ACKNOWLEDGMENTS

Thanks are due to the technical staff (H. Hirt, M. Siemers, and P. Wurster) at the Max-Planck-Institut (Stuttgart) for help with the experiments. We are grateful to R. T. Phillips

for his careful reading and criticism of the manuscript. Special thanks are given to L. C. Lew Yan Voon for providing unpublished results of a tight-binding calculation of MQW's under stress.[24] A.F. acknowledges the Alexander von Humboldt Foundation for financial support in Stuttgart. P.E. and A.S. would like to thank for financial support the European Community (in Cambridge) and the Volkswagen Foundation (in Stuttgart), respectively.

[1] See, for example, J. H. Burnett, H. M. Cheong, W. Paul, E. S. Koteles, and B. Elman, Phys. Rev. B **47**, 1991 (1993).

[2] A painstaking review of the effects of external stresses in semiconductors is given by G. L. Bir and E. Pikus, in *Symmetry and Stress Induced Effects in Semiconductors*, edited by D. Louvish (Wiley, New York, 1974).

[3] For optical experiments under uniaxial stress in MQW's see, for example, H. Quiang, F. Pollak, Kai Shum, Y. Takiguchi, R. R. Alfano, S. F. Fang, and H. Morkoc, Philos. Mag. B **70**, 381 (1994), and references therein.

[4] C. Jagannath, Emil S. Koteles, Johnson Lee, Y. J. Chen, B. S. Elman, and J. Y. Chi, Phys. Rev. B **34**, 7027 (1986)

[5] Johnson Lee, C. Jagannath, M. O. Vassel, and Emil S. Koteles, Phys. Rev. B **37**, 4164 (1988).

[6] Bernard Gil, Pierre Lefebvre, Phillippe Bonnel, Henry Mathieu, Christiane Deparis, Jean Massies, Gérard Neu, and Yong Chen, Phys. Rev. B **47**, 1954 (1993).

[7] Bernard Gil, Pierre Lefebvre, Henry Mathieu, Gloria Platero, Massimo Altarelli, Toshiaki Fukunaga, and Hisao Nakashima, Phys. Rev. B **38**, 1215 (1988).

[8] Johnson Lee, M. O. Vassell, Emil S. Koteles, C. Jagannath, K. T. Hsu, G. J. Jan, C. P. Liu, and I. F. Chang, Phys. Rev. B **40**, 1703 (1989).

[9] A. Fainstein, P. Etchegoin, P. V. Santos, M. Cardona, K. Tötenmayer, and K. Eberl, Phys. Rev. B **50**, 11 850 (1994).

[10] A. Fainstein, P. Etchegoin, M. P. Chamberlain, M. Cardona, K. Tötemeyer, and K. Eberl, Phys. Rev. B **51**, 14 448 (1995).

[11] R. Schorer and G. Abstreiter, Philos. Mag. B **70**, 671 (1994), and references therein.

[12] M. Cardona, in *Atomic Structure and Properties of Solids*, edited by E. Burstein (Academic, New York, 1972), p. 513.

[13] K. Cho, *Excitons* (Springer, New York 1979); Phys. Rev. B **14**, 4463 (1976).

[14] M. Cardona, in *Semiconductors Superlattices and Interfaces*, Proceedings of the International School of Physics ''Enrico Fermi,'' Course CXVII, Varena, 1991, edited by A. Stella and L. Miglio (North-Holland, Amsterdam, 1993), p. 435.

[15] G. D. Sanders and Yia-Chung Chang, Phys. Rev. B **32**, 4282 (1985).

[16] J. M. Luttinger, Phys. Rev. **102**, 1030 (1956).

[17] H. Haug and S. W. Koch, *Quantum Theory of the Optical and Electronic Properties of Semiconductors*, 2nd. ed. (World Scientific, Singapore, 1993).

[18] J. Kircher, W. Böhringer, W. Dietrich, H. Hirt, P. Etchegoin, and M. Cardona, Rev. Sci. Instrum. **63**, 3733 (1992).

[19] The absolute phase of one of the peaks in Fig. 2 is chosen so that the calculated dispersion for $X=0$ coincides with the measurements of the elasto-optic modulator (reflectivity). Once the phase of the peak is identified, the peak is followed for other X's giving the appropriate calibration in each case.

[20] B. Koopmans, B. Richards, P. V. Santos, and M. Cardona (unpublished).

[21] For basic papers on piezobirefringence of semiconductors, see C. W. Higginbotham, M. Cardona, and F. Pollak, Phys. Rev. **184**, 821 (1969); M. Chandrasekhar and F. Pollak, Phys. Rev. B **15**, 2127 (1977); F. H. Pollak and M. Cardona, Phys. Rev. **172**, 816 (1968); P. Etchegoin, J. Kircher, M. Cardona, C. Grein, and E. Bustarret, Phys. Rev. B **46**, 15 139 (1992), and references therein.

[22] R. Sooryakumar, A. Pinczuk, A. C. Gossard, D. S. Chemla and L. J. Sham, Phys. Rev. Lett. **58**, 1150 (1987).

[23] See Fig. 6 of F. Pollak and M. Cardona, Phys. Rev. B **172**, 816 (1968).

[24] L. C. Lew Yan Voon and P. V. Santos (private communication).